***https://doi.org/10.46813/2024-153-124***

# OPTICAL PROPERTIES OF MAGNESIUM-ALUMINUM SPINEL IRRADIATED WITH HIGH-ENERGY ELECTRONS OF THE M-30 MICROTRON

***O. Pop, V.T. Maslyuk, I.G. Megela, V. Roman, I. Pylypchynets, E. Oleinikov, A. Papp***
***Institute of Electron Physics NAS of Ukraine, Uzhhorod, Ukraine***
***E-mail: pop.ksenja@gmail.com***

The study of the optical properties of magnesium-aluminum spinel is relevant because the material has prospects for practical applications and the possibility of use in dosimetry. Therefore, it is important to study the radiation resistance of spinel. This research aims to study the effect of high-energy irradiation, 12.5 MeV, on its optical properties and features of defect formation. It shows that irradiation stimulates the formation of luminescence centers, which is important for solid-state dosimetry. The results indicate the prospects of using non-stoichiometric spinel as a dosimetric material for intense beams of nuclear radiation.

PACS 29.20.-c; 42.25.Bs; 78.55.Ap

## INTRODUCTION

Ionizing nuclear radiation forms the basis of radiation technologies widely used in almost all spheres of human activity – from chemical and pharmaceutical production to space instrumentation. Ionizing radiation is also widely used for sterilization of medical products and materials. Still, its most important use is in the field of nuclear medicine for diagnosis and treatment of diseases. An essential element of such activity is the dosimetric monitoring of the irradiation conditions with beams of nuclear particles of different types and energies, flux densities, and different temperature regimes. This places high demands on the materials of the dosimeters, among which are their radiation resistance, a wide range of fixation of radiation doses, and versatility regarding work in the fields of irradiation with various nuclear particles. Such conditions are satisfied by thermoluminescent (TSL) dosimetry, which is based on the ability of a limited class of broadband crystals to accumulate radiation energy and release it when heated through an optical channel [1].

It is widely used in medical practice, where, along with traditional gamma or electron irradiation procedures, proton and neutron beams and elementary particles of various nature have become widely used [2, 3]. This search for new materials for TSL dosimetry capable of ensuring control of irradiation procedures is urgent. Currently, dosimeters whose active element is lithium fluoride (LiF) are used for dosimetric control tasks. Using the appropriate LiF doping scheme, a whole line of dosimeters has been developed to monitor radiation conditions under the influence of various types of irradiation [3–8]. However, it was established that dosimeters based on these materials have limited application for fixing doses greater than three kGy due to violation of the linearity of the “dose-effect” dependence. In this regard, it is interesting to search for other materials for TL dosimetry with more excellent radiation resistance that can be used to measure higher radiation doses.

Magnesium-aluminum spinel is promising for personal dosimetry, as it is a tissue-equivalent material with an effective atomic number $Z_{eff}$=7, 8, close to its value in biological tissues. It was established that in non-stoichiometric spinel, $MgO{\cdot}2.5Al_2O_3$, linearity of TL output is observed up to $2{\cdot}10^5$Gy. This value is higher than in the traditional materials of TL dosimeters – LiF, $Al_2O_3$ [5, 6, 9–12], which have relatively low radiation resistance, which limits the dose range of their use [9], and the saturation of TL output is observed at doses in 1…2 kGy.

Magnesium-aluminum spinel (MAS) has much higher radiation resistance due to its non-stoichiometric composition, which leads to structural defects that serve as effective getters of radiation defects when the material is irradiated. Magnesium-aluminum spinel crystals, due to their optical and mechanical properties, are promising for their use as optical elements that can work in conditions of radiation fields. In addition, due to their luminescent properties, they can also be used, along with $Al_2O_3$ crystals, for dosimetry of radiation fields (TSL [13, 14], radioluminescence [15–17], optically stimulated luminescence [18, 19]). $MgO{\cdot}2.5Al_2O_3$ spinels demonstrate high radiation resistance in terms of mechanical characteristics even under powerful neutron irradiation [4], due to structural defects-getters and low efficiency of accumulation of radiation-displaced atoms.

The study of radiation defects in spinel crystals of various compositions irradiated by reactor neutrons with fluences of $10^{18}$ n/cm$^2$ accompanied by gamma quanta was studied in [20–22] and formed during electron gamma irradiation of 16 MeV [20, 21]. Further prospects for using these materials require understanding the nature of the substance's resistance to radiation, studying the nature of radiation defect formation under the action of nuclear particles of various natures, and comparing their characteristics with other dosimetric materials.

Despite many publications devoted to the effect of radiation on the characteristics of spinel crystals, the nature of their radiation defect formation and sensitivity to ionizing radiation has practically yet to be studied. The high structural defectiveness of such materials, due to the presence of additional cationic vacancies, contributes to the formation of optical centers of various natures by capturing charge carriers formed upon irradiation with these defects or impurity atoms.

In this work, the results of the study of the effect of irradiation with high-energy (12.5 MeV) electrons of the M-30 microtron on the optical properties of magnesium-aluminum spinel $MgO{\cdot}2{,}5Al_2O_3$, and the study of the dose dependence of the formation of its optical centers are presented.

## 1. THE RADIATION EXPERIMENT

The studied samples were irradiated on the M-30 microtron of the Institute of Electronic Physics of the National Academy of Sciences of Ukraine, which certifies the radiation resistance of materials and equipment. The microtron radiation pulse is a sequence of electron bunches that follow each other with a frequency of 3200 MHz and a duration of 30 ps. The average current of the electron beam can vary from 0.01 to 50 μA with a current of accelerated electrons in a pulse of up to 50 mA, a current pulse duration of 0.15…0.20 μs with a pulse repetition frequency of 1 kHz. A specially prepared metrological stand was used to experiment, the parameters of which are parameterized according to the density of the flow of accelerated electrons and the uniformity of the irradiation field through each meter. A special former was used to ensure uniformity of the irradiation field and better concentration of the electron beam [23]. The general appearance of the M-30 microtron, a metrological stand for radiation experiments, is shown in Fig. 1.

*Fig. 1. The M-30 microtron as a metrological test bench for radiation experiments*

The irradiation process involves preliminary control of the density of the flow of accelerated electrons on the irradiation plane using a Faraday cylinder (F), which has a calibrated window diameter of 50 mm. The data obtained from the CF are harmonized with the readings of the secondary emission monitor (SEM), which directly records the current of accelerated electrons at the output of the M-30 and is connected to the current integrator. Based on these measurements, the SEM was calibrated, and its indicators were output to the automated control panel to determine the integral fluence and the absorbed dose. A copper-constantan thermocouple controlled the temperature of the samples during irradiation. The beam of accelerated electrons at the exit from the M-30 has dimensions of 1 $cm^2$, with a current of 3…5 μA, the flux density at a distance of 0.6 m from the output window, where the samples were placed, varied between $1.0{\cdot}10^{10}…3.0{\cdot}10^{13}$ $el{\cdot}cm^{-2}{\cdot}s^{-1}$ [24]. When irradiation leads to heating of the samples, they were cooled in liquid nitrogen vapor to ensure the optimal temperature, around 20 °C. The required temperature of the samples was maintained by adjusting the intensity of nitrogen evaporation and controlling the heating of the samples with a copper-constantan thermocouple. For the conditions of this experiment, the energy of the accelerated electrons was 12.5 MeV, and the fluence, or the sample irradiation dose, varied between $10^{12}$ and $10^{16}$ $el{\cdot}cm^{-2}$.

## 2. OPTICAL MEASUREMENTS

Measurements of the optical transmittance of MAS were carried out on an SF-46 spectrophotometer in the wavelength range of 200…1000 nm. As a source, a deuterium lamp designed for operation in the spectrum range from 190 to 350 nm, and an incandescent lamp for the spectrum range from 340 to 1100 nm was used. Spectra were recorded using an antimony-cesium photocell up to 650 nm and an oxygen-cesium photocell starting at 650 nm.

Measurements of phosphorescence and thermoluminescence were carried out on the device, the capabilities of which are described in [25]. A FEU-136 photomultiplier in photon counting mode was used to measure the intensity of luminescence. The thermoluminescence curves were obtained due to linear heating of the studied samples at a rate of 1 °C/s to the maximum temperature of 300 °C. To prevent unwanted red and IR radiation from entering the entire surface of the heater to the entrance window of the FEP, the film structure was covered with a diaphragm with an opening of ∅5 mm, and a blue-green light filter of the SZS-21 type was also used. The temperature of the samples was controlled using chrome-drop thermocouples with an ultra-small working junction volume.

## 3. RESULTS AND DISCUSSION

The interaction of nuclear radiation with matter is accompanied by the accumulation of radiation energy through the activation of ionization centers and radiation defect formation. The first of these mechanisms is used in solid-state dosimetry when thermally stimulated luminescence (TSL) releases the accumulated radiation energy. As a rule, wide-gap semiconductors are used as dosimetric materials. TSL is carried out through radiative transitions to local energy levels in the band gap, the structure of which is formed by doping or technological defects [2, 26–29]. Radiation defects formed during the irradiation of semiconductors can change the structure of local energy levels, affecting the sensitivity and the material's ability to set the absorbed dose and store data on its value. Therefore, control of the type and concentration of radiation defects introduced by the action of high-energy nuclear particles is an essential task of solid-state dosimetry.

The study of optical spectra of the samples is widely used to identify radiation defects in MAS crystals. In the literature, there is data on such studies performed on samples irradiated in electron beams [20, 30–32], gamma quanta [31], and neutrons [31–35]. As a rule, the optical transmittance of samples [20, 21, 36], which contains two broad absorption bands in the intervals of

3.1 and 5 eV, is studied to identify anionic vacancies in spinel and establish their concentration. It is believed [30, 31, 37] that the absorption band at 3.1 eV is due to vacancies of $Mg^{2+}$ and $Al^{3+}$ cations, which are hole traps – V-centers, and at 5 eV, it is formed by electron traps associated with oxygen vacancies in tetra positions F (anion vacancies captured two electrons) and octa $F^+$ (anion vacancies captured one electron).

Fig. 2 shows the results of studying the optical absorption of spinel samples irradiated in the fluence range of $10^{14}…10^{16}$ el·cm$^{-2}$ corresponds to absorbed radiation doses from 30 kGy to 3 MGy.

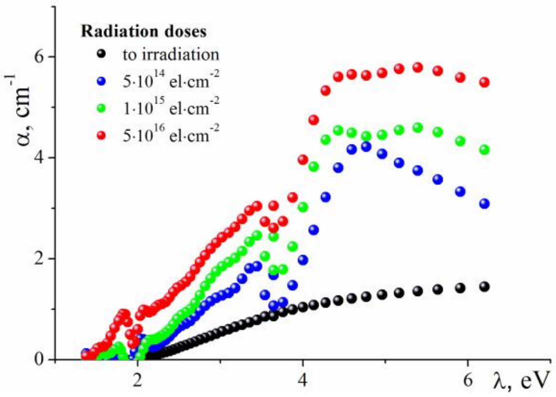


*Fig. 2. Absorption spectra of $MgO·2.5Al_2O_3$ spinel samples as a function of irradiation dose obtained by electron beams with an energy of 12.5 MeV. Electron flux densities for the given radiation doses are shown in the article*

Such measurements have their peculiarities since the samples immediately after irradiation show significant phosphorescence, and for measurements, it takes time for them to fade. The different electron flux densities of the M-30 microtron provided a wide range of MASH irradiation doses. Thus, to obtain a fluence of $5·10^{14}$ el·cm$^{-2}$, the flux density was $6.7·10^{10}$ el·cm$^{-2}$·s$^{-1}$, for fluences of $5·10^{15}$ and $5·10^{16}$ el·cm$^{-2}$, respectively, $3·10^{13}$ el·cm$^{-2}$·s$^{-1}$, the conditions of irradiation at high fluxes were provided by cooling with liquid nitrogen vapors.

As can be seen, the absorption spectra of MAS crystals before irradiation do not have visible bands in the entire spectral range, which indicates a high level of purity of the crystals. MAS irradiation results in the appearance and growth of absorption in the range of 0.5…6.5 eV, which is consistent with similar studies by other authors [20, 21]. It can be seen that the degree of radiation-induced absorption, which is formed by the overlap of two broad bands centered around 3.1 and 5 eV, increases with the radiation dose. Such bands do not depend on the irradiation conditions, as indicated in works [31–33, 37–39]. In contrast to the results presented in [21], where the irradiation temperature was 200 °C, in our case, irradiation in a direct beam was carried out at room temperature due to cooling with vapors of liquid nitrogen.

Fig. 3 shows the dependence of the optical absorption coefficient on the irradiation dose for the 5 eV band. This band shows a more significant increase, indicating a higher formation rate of anion vacancies associated with oxygen vacancies, F centers, during irradiation.

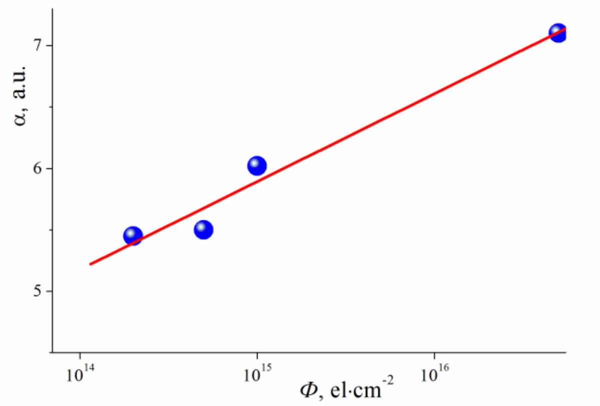


*Fig. 3. Dependence of the optical absorption coefficient MAS for the 5 eV band on the irradiation dose. Irradiation conditions are shown in the previous figure*

The obtained results contrast with the data of the study of optical absorption in $Al_2O_3$ crystals irradiated under similar conditions to achieve high doses of radiation (Fig. 4). With a set of fluences of $8·10^{14}$ and $10^{15}$ el·cm$^{-2}$, the flux density was $5·10^{12}$ el·cm$^{-2}$·s$^{-1}$ with the sample cooling in sharp nitrogen vapors. As can be seen, the result of irradiation is not an increase but a decrease in optical absorption in this spectral range.

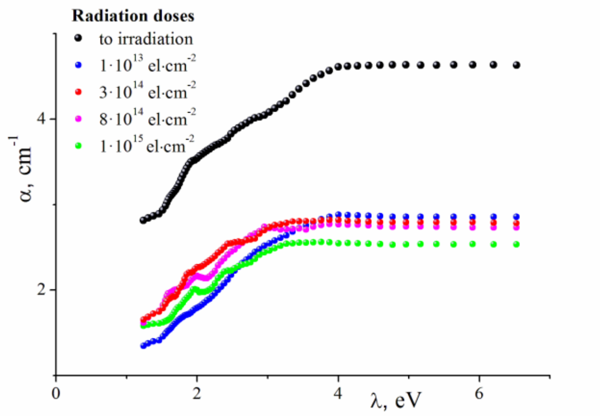


*Fig. 4. Absorption spectra of $Al_2O_3$ samples from the irradiation dose for the energy of accelerated electrons of 12.5 MeV. Electron flux densities for the given radiation doses are shown in the article*

This phenomenon is most likely related to the effect of radiation "healing" structural defects, the effect of small doses [40, 41], and the restoration of the crystal's structural perfection due to the reduction of the number of existing technological, uncontrolled defects as a result of radiation-stimulated diffusion.

*Phosphorescence.* As mentioned above, long-term phosphorescence occurs due to the irradiation of the studied samples. Fig. 5 shows the kinetics of phosphorescence decay of samples irradiated with fluences from $10^{12}$ to $5·10^{14}$ el·cm$^{-2}$ at electron flux densities of $6.7·10^{10}$ el·cm$^{-2}$·s$^{-1}$, which did not require cooling the samples in liquid nitrogen vapor.

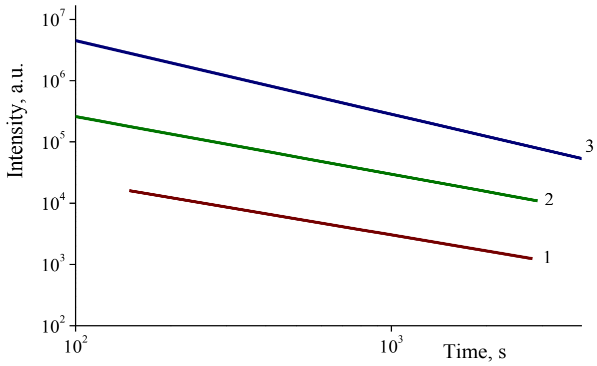


*Fig. 5. Kinetics of phosphorescence decay in MAS samples irradiated with a flow of electrons with a density of 6.7·$10^{10}$ el·$cm^{-2}$·$s^{-1}$: 1 – corresponds to an electron fluence of 1·$10^{12}$ el·$cm^{-2}$, respectively; 2 – 2·$10^{14}$ el·$cm^{-2}$ and 3 – 5·$10^{14}$ el·$cm^{-2}$*

The action of ionizing radiation leads both to the formation of luminescence centers due to the localization of charge carriers on trap levels and to radiation defects of the type of displaced atoms – the result of an elastic collision of relativistic electrons with atoms of the environment. The resulting radiation defects can be found in new luminescence and non-radiative recombination centers. It was established that the phosphorescence of irradiated spinel crystals, Fig. 5, differs significantly from the kinetics of phosphorescence decay of other dosimetric materials, such as LiF: Mg, Cu, P, and $Al_2O_3$, irradiated under similar conditions [5, 9]. These differences are manifested in the dose dependence of their intensities. The obtained data testify in favor of the fact that radiation defects in spinel crystals are additional centers of radiative recombination, i.e., during irradiation, the concentration of the activator of luminescent processes [42] and the intensity of phosphorescence increase.

*Thermoluminescence.* Typical thermoluminescence spectra of the same samples after the decay of the phosphorescence signal are shown in Fig. 6. The curves are built using attenuating filters – a blue-green light filter of the SZS-21 type and a special diaphragm that weakens the intensity of TSL. As can be seen from Fig. 6, one dominant peak of TSL, located around 160…170 °C, was found in the studied samples, the position of which does not change under the influence of the absorbed radiation dose within 10%.

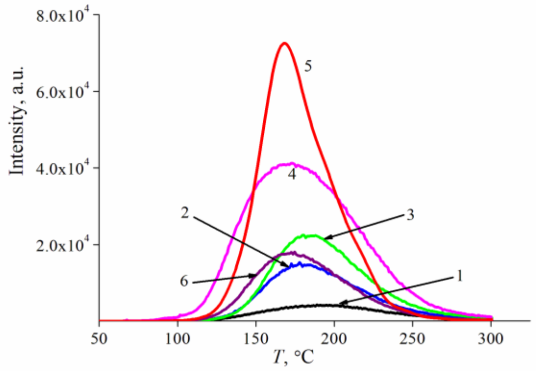


*Fig. 6. TSL curves of irradiated samples: 1 – 1·$10^{12}$ el·$cm^{-2}$; 2 – 1·$10^{13}$ el·$cm^{-2}$; 3 – 5·$10^{13}$ el·$cm^{-2}$; 4 – 1·$10^{14}$ el·$cm^{-2}$; 5 – 5·$10^{14}$ el·$cm^{-2}$; 6 – 5·$10^{16}$ el·$cm^{-2}$*

As shown in Fig. 6, as the radiation dose increases, the output of the peak light sum and the value of its maximum increase. The results of the study of the total yield of the total volume of TSL depending on the radiation dose are shown in Fig. 7.

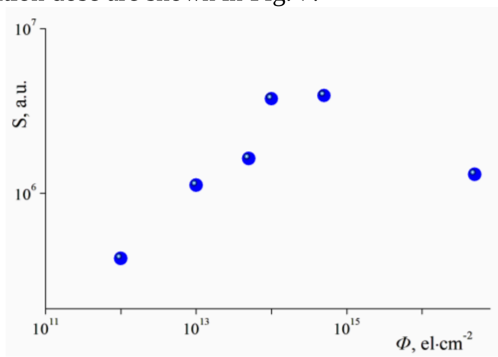


*Fig. 7. Dependence of the total output of TSL on the fluence of electrons*

As can be seen, the maximum output of the amount of TSL is observed at fluences of 5·$10^{14}$ el·$cm^{-2}$, and there is an almost linear dependence of its value on the radiation dose. The value of the maximum output of the TSL sum is significantly higher than that for widely used NCP dosimeters [43, 44], where saturation is observed at fluences of 1·$10^{13}$ el·$cm^{-2}$. This indicates the possibility of using MAS as dosimeters of powerful radiation fields and for technological dosimetry of nuclear and power plants. The data shown in Fig. 6 can be used to estimate the activation energy, the order of luminescence kinetics, and the frequency factor using the computerized glow curve deconvolution (CGCD) method, which is widely used in dosimetric studies [45]. This happens by fitting the experimental data with model dependencies in the assumed luminescence kinetics of the first, second, or arbitrary order. Estimates show that for non-stoichiometric MAS, the position of the dosimetric peak, Fig. 6, due to the presence of deep traps, the activation energy of which in the band gap is 0.9 eV, and their frequency factor is estimated at $10^6$ $s^{-1}$. The obtained data compare quite well with the available literature sources. More accurate values can be obtained in a series of TSL experiments with different sample heating rates.

## CONCLUSIONS

This work presents a systematic study of the influence of nuclear irradiation on the optical properties of the MAS obtained in a series of experiments on the M-30 microtron. The possibility of identifying and controlling the defect state of spinel crystals by optical methods is shown, as well as establishing the nature of radiation defect formation under the action of intense beams of high-energy electrons. The presented results relate to the optical characteristics of MAS MgO·2.5$Al_2O_3$ crystals irradiated on the M-30 microtron; the subject of the study were light transmission indicators, as well as luminescent characteristics – spontaneous and long-term phosphorescence, as well as TSL. It is shown that the latter characteristics allow controlling the state of the structure of the local spinel energy levels in the band gap of the crystal, which provides information about its defectivity and radiation resistance. The results are compared with the data of similar experiments conducted for dosimetric materials based on leucosapphire, $Al_2O_3$, and lithium fluoride, LiF. It is shown that the difference in the structural structure of, for example, MAS and $Al_2O_3$ leads to different behavior of their optical characteristics under irradiation – photobrightening for leucosapphire and photodarkening for spinel.

Moreover, a stronger dependence of photodarkening on the irradiation dose is observed for MAS. For spinel crystals, the role of structural vacancies caused by $Mg^{2+}$ and $Al^{3+}$ cations, which are hole traps – V-centers and electron traps associated with oxygen vacancies in tetra- and octa-F positions during radiation modification of their optical characteristics, has been established. These materials' established types of structural defects may be responsible for the structure of local energy levels in the band gap and features of luminescent phenomena such as TSL and phosphorescence. It is shown that $MgO·2.5Al_2O_3$ spinel crystals are significantly more radiation-resistant concerning changes in their optical characteristics, as evidenced by both phosphorescence and TSL data, which makes it possible to develop thermoluminescent sensors based on them for clinical and technological dosimetry. However, the use of spinel $MgO·2.5Al_2O_3$ for radiation-resistant windows is less promising than leucosapphire $Al_2O_3$ since their optical properties degrade in the fields of ionizing radiation.

## ACKNOWLEDGEMENTS

The work was partially carried out within the framework of Grants of the NAS of Ukraine to research laboratories/groups of young scientists of the NAS of Ukraine for conducting research in the priority directions of the development of science and technology in 2024-2025. State registration number – 0124U001974.

## REFERENCES

1. K. Shinsho. *Thermally Stimulated Luminescent (TSL) Materials. In Phosphors for Radiation Detectors* / Eds. T. Yanagida and M. Koshimizu. 2022; https://doi.org/10.1002/9781119583363.ch7

2. S.W. McKeever, M. Moscovitch, and P.D. Townsend. *Thermoluminescence Dosimetry Materials: Properties and Uses*. United Kingdom: Nuclear Technology Publishing, 1995.

3. G. Okada, Y. Koguchi, T. Yanagida, S. Kasap, and H. Nanto. Recent advances in radiophotoluminescence materials for luminescence dosimetry // *Japanese Journal of Applied Physics*. 2023, v. 62 (1), p. 010609; https://doi. org/10.35848/1347-4065/ac9023

4. Y.S. Horowitz, S. Mahajna. The unified interaction model applied to the gamma induced supralinearity and sensitisation of peaks 4 and 5 in LiF:Mg,Ti (TLD-100) // *Radiat. Prot. Dosimetry*. 1999, v. 84, p. 29-34.

5. V.T. Maslyuk, I.G. Megela, B. Obryk, T.O. Vieru-Vasilitsa. Luminescent properties of LiF:Mg,Cu,P detectors irradiated by the 10-MeV electrons // *Radiation effects & defects in solids*. 2017, v. 172 (9-10), p. 782-789; https://doi:10.1080/10420150.2017.1393425

6. P. Bilski, B. Obryk, W. Gieszczyk, P. Baran. Position of LiF:Mg, Cu, P TL peak as an alternative method for ultra-high-dose dosimetry // *Radiation Measurements*. 2020, v. 139, p. 106486; https://doi.org/10.1016/j.radmeas.2020.106486

7. V. D'Avino, M. Caruso, C. Arrichiello, G. Ametrano, and G. La Verde. Thermoluminescent dosimeters (TLDs-100) calibration for dose verification in photon and proton radiation therapy // *IL Nuovo Cimento C*. 2020, v. 43, p. 1–11; DOI 10.1393/ncc/i2020-20142-0

8. S. Motta, J.B. Christensen, M. Togno, R. Schä-fer, S. Safai, A.J. Lomax, and E.G. Yukihara. Characterization of LiF:Mg,Ti thermoluminescence detectors in low-LET proton beams at ultra-high dose rates // *Phys. Med. Biol*. 2023, v. 68, p. 045017; DOI 10.1088/1361-6560/acb634

9. V.T. Maslyuk, I.G. Megela, T.O. Okunieva, J.M. Pekar, V.J. Pekar. Specific features of the influence of high-energy electron beams on the luminescent properties of undoped and Nb, Fe-doped $Al_2O_3$ crystals // *Radiation Protection Dosimetry*. 2014, v. 162 (1-2), p. 34; https://doi.org/10.1093/rpd/ncu213

10. L. Cain, G. Pogatshnik, Y. Chen. Optical transitions in neutron-irradiated $MgAl_2O_4$ spinel crystals // *Phys. Rev. B.* 1988, v. 37 (5), p. 2645-2652; https://doi.org/10.1103/PhysRevB.37.2645

11. J.B. Christensen, M. Togno, K.P. Nesteruk, S. Psoroulas, D. Meer, D.C. Weber, T. Lomax, E.G. Yukihara, and S. Safai. $Al_2O_3$:C optically stimulated luminescence dosimeters (OSLDs) for ultra-high dose rate proton dosimetry // *Phys. Med. Biol*. 2021, v. 66, p. 085003; DOI: 10.1088/1361-6560/abe554

12. R. Kranzer, A. Schüller, A. Bourgouin, T. Hackel, D. Poppinga, M. Lapp, H.K. Looe, and B. Poppe. Response of diamond detectors in ultrahigh dose-per-pulse electron beams for dosimetry at FLASH radiotherapy // *Phys. Med. Biol*. 2022, v. 67, p. 075002; DOI: 10.1088/1361-6560/ac594e

13. F.A. Garner, G.W. Hollenberg, F.D. Hobbs, J.L. Ryan, Z. Li, C.A. Black, R.C. Bradt. Dimensional stability, optical and elastic properties of $MgAl_2O_4$ spinel irradiated in FFTF to very high exposures // *Journal of Nuclear Materials*. 1994, v. 212-215, p. 1087-1090; https://doi.org/10.1016/0022-3115(94)91000-6

14. Taekyu Kim, Hyunshik Kang, Jeongjoo Woo, Kisoo Chung and Hongsoo Choe. Hongkyu Jang and Chungnam Whang Thermoluminescence of Magnesium Aluminum Spinel // *Journal of the Korean Physical Society*. 1999, v. 34 (4), p. 385-389.

15. O.K. Tyutyunik, A.O. Moskvitin, Yu.G. Ka-zarinov, V.T. Gritsyna. Radioluminescence mechanism of magnesium aluminate spinel in transparent ceramics // *Functional Materials*. 2010, v. 17 (1), p. 41-45; http://dspace.nbuv.gov.ua/handle/123456789/134166

16. V. Gritsyna, Yu. Kazarinov. Effects of transition-metal-doping on the radio-luminescence

properties of magnesium aluminate spinel crystals // *Rad. Applic*. 2018, v. 3 (1), p. 7–12; doi:10.21175/RadJ.2018.01.002

17. V.T. Gritsyna, Yu.G. Kazarinov, V.A. Kobyakov, I.E. Reimanis. Radiation-induced luminescence in magnesium aluminate spinel crystals and ceramics // *Nuclear Instruments and Methods in Physics Research Section B: Beam Interactions with Materials and Atoms.* 2006, v. 250(1-2), p. 342-348; https://doi.org/10.1016/j.nimb.2006.04.135

18. E.G. Yukihara, S.W.S. Mckeever. *Optically Stimulated Luminescence: Fundamentals and Applications*. John Wiley & Sons, 2011.

19. E.M. Yoshimura, E.G. Yukihara. Optically stimulated luminescence of magnesium aluminate ($MgAl_2O_4$) spinel // *Radiation Measurements.* 2006, v. 4, p. 163-169; doi:10.1016/j.radmeas.2005.09.001

20. S.P. Gokov, V.T. Gritsyna, S.S. Kochetov, V.I. Kasilov, Yu.G. Kazarinov. Defects formation in spinel crystals under electron and gamma beam irradiation // *Problems of Atomic Science and Technology.* 2009, N 5(93), p. 43-45; http://dspace.nbuv.gov.ua/handle/123456789/111120

21. Yu.G. Kazarinov, V.T. Hrytsyna, V.A. Kobyakov, K.E. Sikafus. Luminescent properties of spinel single crystals under the influence of ionizing radiation // *Problems of Atomic Science and Technology.* 2002, N 3, p. 53-57; http://dspace.nbuv.gov.ua/handle/123456789/80084

22. F.W. Clinard, G.F. Hurley, L.W. Hobbs. Neutron irradiation damage in MgO, $Al_2O_3$ and $MgAl_2O_4$ ceramics // *Journal of Nuclear Materials*. 1982, v. 108-109, p. 655-670; https://doi.org/10.1016/0022-3115(82)90538-4

23. M.I. Romanyuk, J.J. Hainysh, Y. Plakosh, V. Kovtun, O.M. Turhovsky, G.F. Pitchenko, I.G. Megela, M.V. Goshovsky, O.O. Parlag, V.T. Maslyuk, N.I. Svatiuk. Microtron M-30 for radiation experiments: formation and control of irradiation fields // *Problems of Atomic Science and Technology*. 2022, N 3, p. 137-143; https://doi.org/10.46813/2022-139-137

24. V. Maslyuk, O. Pop, B. Obryk, N. Svatiuk, J. Hainish, A. Rusyn, M. Romanyuk, I. Megela. Dosimetric studies of e-, γ-, n-irradiation fields of the M-30 microtron (18.5 MeV) // *Radiation Physics and Chemistry*. 2024, v. 223, p. 111964; https://doi.org/10.1016/j.radphyschem.2024.111964

25. V.I. Lyamayev. A low-cost microcontroller-based measurement system for a fractional glow technique // *Meas. Sci. Technol*. 2006, v. 17, p. 75; DOI 10.1088/0957-0233/17/12/N01

26. V. Kortov. Materials for thermoluminescent dosimetry: Current status and future trends // *Radiation Measurements*. 2007, v. 42 (4-5), p. 576; https://doi.org/10.1016/j.radmeas.2007.02.067

27. A. Duragkar, A. Muley, N.R. Pawar, V. Chopra, N.S. Dhoble, O.P. Chimankar, S.J. Dhoble. Versatility of thermoluminescence materials and radiation dosimetry – A review // *Luminescence*. 2019, v. 34(7), p. 656; https://doi.org/10.1002/bio.3644

28. S. Chand, R. Mehra, V. Chopra. Recent developments in phosphate materials for their thermoluminescence dosimeter (TLD) applications // *Luminescence*. 2021, v. 36, p. 1808; https://doi.org/10.1002/bio.3960

29. D. Kural, E. Ekdal Karal, A. Kelemen, V. Holovey, N. Can, T. Karal. Thermoluminescence characterization of Ag-doped $Li_2B_4O_7$ single crystal materials // *Luminescence*. 2017, v. 32 (5), p. 786; https://doi.org/10.1002/bio.3252

30. Y. Kazarinov, I. Megela, and O. Pop. Monitoring of Radiation Defects Recovery in $MgAl_2O_4$ During Annealing by Optical Spectroscopy // *East European Journal of Physics.* 2023, v. 1, p. 130-134; https://doi.org/10.26565/2312-4334-2023-1-16

31. J. Bunch. Mollwo-Ivey relation between peak color-center absorption energy and average oxygen ion spacing in several oxides of group-II and -III metals // *Phys. Rev. B*. 1977, v. 16 (2), p. 724-725; https://doi.org/10.1103/PhysRevB.16.724

32. G. Summers, G. White, K.H. Lee, J.H. Crawford. Radiation damage in $MgAl_2O_4$ // *Phys. Rev. B.* 1980, v. 21 (6), p. 2578-2584; https://doi.org/10.1103/PhysRevB.21.2578

33. L. Cain, G. Pogatshnik, Y. Chen. Optical transitions in neutron-irradiated $MgAl_2O_4$ spinel crystals // *Phys. Rev. B*. 1988, v. 37 (5), p. 2645-2652; https://doi.org/10.1103/PhysRevB.37.2645

34. A. Lushchik, S. Dolgov, E. Feldbach, R. Pareja, A.I. Popov, E. Shablonin, V. Seeman. Creation and thermal annealing of structural defects in neutron-irradiated $MgAl_2O_4$ single crystal // *Nucl. Instrum. Methods Phys. Res. B*. 2018, v. 435, p. 31-37; doi:10.1016/j.nimb.2017.10.018

35. A. Lushchik, E. Feldbach, E.A. Kotomin, I. Kudryavtseva, V.N. Kuzovkov, A.I. Popov, V. Seeman, E. Shablonin. Distinctive features of diffusion-controlled radiation defect recombination in stoichiometric magnesium aluminate spinel single crystals and transparent polycrystalline ceramics // *Sci. Rep.* 2020, v. 10, p. 7810; doi:10.1038/s41598-020-64778-8

36. S. Yoshioka, K. Tsuruta, T. Yamamoto. Local structure investigations of accumulated damage in irradiated $MgAl_2O_4$ // *J. Am. Ceram. Soc.* 2020, v. 103, p. 4654-4663; https://doi.org/10.1111/jace.17101

37. Yu.H. Kazarinov, O.M. Pop, I.G. Megela, A.I. Popov. Effect of electron irradiation conditions on the efficiency of defect formation in $MgAl_2O_4$ spinel // *Problems of Atomic Science and Technology*. 2022, N 5 (141), p. 25-28; https://doi.org/10.46813/2022-141-025

38. A. Ibarra, F.J. Lopez, M. Jimenez de Castro. V centers in $MgA1_2O_4$ spinels // *Physical Review B*. 1991, v. 44 (14): p. 7256-7262; DOI: 10.1103/physrevb.44.7256

39. A. Ibarra, D.F. Mariani and M. Jiménez de Castro. Thermoluminescent processes of $MgAl_2O_4$ irradiated at room temperature // *Phys. Rev. B*. 1991, v. 44, p. 12158; https://doi.org/10.1103/PhysRevB.44.12158

40. M. Carrard, D. Emin, and L. Zuppiroli. Defect clustering and self-healing of electron-irradiated boron-rich solids // *Phys. Rev. B.* 1995, v. 51, p. 11270; https://doi.org/10.1103/PhysRevB.51.11270

41. Kazunori Fujisawa, Bruno R Carvalho, Tianyi Zhang, Néstor Perea-López, Zhong Lin, Victor Carozo, Sérgio LLM Ramos, Ethan Kahn, Adam Bolotsky, He Liu, Ana Laura Elías, and Mauricio Terrones. Quantification and Healing of Defects in Atomically Thin Molybdenum Disulfide: Beyond the Controlled Creation of Atomic Defects // *American Chemical Society Nano*. 2021, v. 15 (6), p. 9658-9669; doi: 10.1021/acsnano.0c10897

42. A. Vedda, M. Fasoli. Tunneling recombinations in scintillators, phosphors, and dosimeters // *Radiation Measurements.* 2018, v. 118, p. 86-97; https://doi.org/10.1016/j.radmeas.2018.08.003

43. Barbara Obryk, Paweł Bilski, Krzysztof Hodyr, Patrycja Mika. *The Second International Conference on Radiation and Dosymetry in Various Fields of Research (RAD 2014)* / Ed. by Goran Ristić. Niš: Faculty of Electronic Engineering (Niš: Faculty of Electronic Engineering, 2014), p. 207; (http://www.rad2014.elfak.rs/php/download2.php?file=../prezentacije/Book%20of%20Abstracts%20RAD%202014.pdf)

44. Mária Ranogajec-Komor. Thermoluminescence Dosimetry-Application in Environmental Monitoring // *Radiation Safety Management.* 2003, v. 2 (1), p. 2; DOI: 10.12950/rsm2002.2.2

45. L. Robindro Singh, S. Dorendrajit Singh, and T. Dwijen Singh. CGCD technique to find the kinetic parameters of TL glow curves // *Sci. Vis.* 2011, v. 11 (4), p. 179-184; https://api.semanticscholar.org/CorpusID:17939723

*Article received 25.09.2024*

## ОПТИЧНІ ВЛАСТИВОСТІ МАГНІЄВО-АЛЮМІНІЄВОЇ ШПІНЕЛІ, ОПРОМІНЕНОЇ ВИСОКОЕНЕРГЕТИЧНИМИ ЕЛЕКТРОНАМИ МІКРОТРОНУ М-30

***О. Поп, В.Т. Маслюк, І.Г. Мегела, В. Роман, І. Пилипчинець, Є. Олейников, А. Папп***

Дослідження оптичних властивостей магнієво-алюмінієвої шпінелі є актуальними, оскільки матеріал має перспективи практичного застосування та можливість використання у дозиметрії. Тому важливо дослідити радіаційну стійкість шпінелі. Ці дослідження спрямовані на вивчення впливу високоенергетичного опромінення 12,5 МеВ на його оптичні властивості та особливості дефектоутворення. Показано, що опромінення стимулює утворення центрів люмінесценції, що важливо для твердотільної дозиметрії. Отримані результати свідчать про перспективність використання нестехіометричної шпінелі як дозиметричного матеріалу для інтенсивних пучків ядерного випромінювання.